Materials Research. 2025; 28:e20240308
DOI: https://doi.org/10.1590/1980-5373-MR-2024-0308

Study of the efficacy of Zinc Oxalate Conversion Coating in Protecting Structures Containing Galvanized Steel in Corrosive Environments with ph Variation

***Tatiana C.M. Barretto*[a*], *Carlos A.C. Souza*[b], *José M. Ferreira Jr.*[c], *Daniel V. Ribeiro*[b]**

[a]*Universidade Federal da Bahia, Programa de Pós-Graduação em Engenharia Civil (PPEC), Rua Aristides Novis, 02, 40210-630, Salvador, BA, Brasil.*
[b]*Universidade Federal da Bahia, Departamento de Ciência e Tecnologia dos Materiais, Rua Aristides Novis, 02, 40210-630, Salvador, BA, Brasil.*
[c]*Iowa State University of Science and Technology, Department of Chemistry 2433, 50001, Union Drive, Ames, United States.*

Received: July 18, 2024; Revised: October 31, 2024; Accepted: January 07, 2025

Corrosion of reinforcing bars in reinforced concrete significantly compromises the durability of structures. In aggressive environments, measures such as galvanization are common, but surface treatments with zinc chromate (Cr^{6+}), a carcinogenic compound, demand safer alternatives. Organic acids, especially oxalic acid, have shown promise in acidic environments, but their efficacy under alkaline conditions is uncertain. This study evaluates the zinc oxalate conversion coating on galvanized steel exposed to corrosive environments with varied pH. Galvanized sheets were treated with oxalic acid [0.1 m] and exposed to alkaline solutions (pH 13) and slightly acidic nacl solutions (ph 6.5). Corrosion resistance tests and analyses of phase formation (XRD) and morphology (SEM) were conducted. Results showed that the zinc oxalate film acts as a physical barrier in acidic conditions but dissolves in alkaline environments, demonstrating ineffectiveness. In NaCl solution, treatment with oxalic acid promotes the formation of a zinc oxalate layer, which accelerates the formation of corrosion products and improves resistance to corrosive attack. In contrast, treatment with an alkaline solution results in a less effective passivation layer, offering limited protective effects and leading to a higher corrosion rate over time.

Keywords: *Corrosion, Reinforcement, Electroplating, Oxalic Acid, Surface Treatment.*

1. Introduction

The good quality of concrete, adequate cover thickness, and correct execution are not sufficient conditions to guarantee adequate protection of reinforcement in structures exposed to aggressive environments rich in chlorides. In these environments, corrosive agents can access the reinforcement through pores existing in the concrete and through cracks resulting from mechanical stresses, which can lead to severe corrosion.

The use of additional protection measures will increase construction costs, but, in the long run, maintenance costs and future shutdowns due to equipment failure caused by corroded structures will be reduced[1,2].

There are many protection measures to prevent reinforcement corrosion in concrete structures, such as: the use of corrosion inhibiting additives, cathodic protection of reinforcement, coating the reinforcement with a zinc-based or polymer layer deposit, replacing carbon steel reinforcement with corrosion-resistant materials, and coating the concrete with protective coverings[3-8].

Many techniques are used to coat reinforcements, such as galvanic coatings that use metals nobler than steel. Among these metals, zinc is the most widely used due to its properties: the ability to form a dense and adherent protective film on the reinforcement surface, allowing the corrosion rate to decrease compared to that of other ferrous oxides[9]. Zinc protects steel against corrosion through cathodic protection and, for this reason, is widely employed to coat or galvanize ferrous metal products[10-12].

One of the prerequisites for the atmospheric corrosion of zinc is that a layer of moisture be present, acting as a solvent for atmospheric constituents and as a medium for electrochemical reactions to occur. When the moisture layer evaporates, a film of corrosion products precipitates, and the nature of these precipitates depends on the environmental characteristics of the atmosphere[10].

The chemical composition of corrosion product layers changes with exposure time and is not uniform throughout its thickness. Thus, some phases appear after short exposure periods, while others are found only after longer exposures[10].

The corrosion rate will be closely linked to the exposure time, probably due to the formation of corrosion products adhering to the surface, as these corrosion products become denser with continuous exposure, thus providing a thicker and more protective layer[10].

Zinc is an amphoteric transition metal, meaning it can react with acidic or basic behavior to form divalent salts. Thus, the way zinc corrosion will occur mainly depends on the pH of the environment. In strongly acidic or highly

*e-mail: tatibarretto@hotmail.com

alkaline environments, zinc corrodes at a very high rate. In acidic pH environments, corrosion is the product of the anodic reaction of zinc cations (Zn^{2+}), whereas in neutral or slightly alkaline pH environments, the main corrosion product is zinc hydroxide or zinc complexes that depend on the zinc coordination atom and pH value[13].

For zinc-coated steel inserted in an alkaline environment, the corrosion behavior will be influenced not only by the pH value of the medium but also by the presence or absence of calcium cations, Ca^{2+}[13].

Surface treatments are commonly used to increase the corrosion resistance of steel, with chromating standing out[14-16] However, this treatment generally involves the presence of hexavalent chromium ions (Cr^{6+}), which are highly toxic, being a carcinogenic agent that can have serious negative consequences for workers and users. The high toxicity has led to its suspension in some countries[17,18], increasing the need to replace hexavalent chromium in conversion solution immersion treatments.

In recent years, several researchers[18-20] have sought alternative coatings that provide corrosion resistance comparable to chromate coatings. Among these alternatives is the application of organic acids, especially dicarboxylic acids, an economically viable option for increasing the corrosion resistance of metal substrates because it is a simpler and lower-cost treatment compared to conventional ones[19-22]. Among the organic acids, the simplest of them, oxalic acid or ethanedioic acid, has been widely used due to its high capacity to remove iron oxides and encrusted impurities[20,21,23-25].

This study proposes to evaluate the efficiency of zinc oxalate conversion coating on substrates exposed to different corrosive environments, alkaline solutions, and solutions containing NaCl, with pH values of 13.0 and 6.5, respectively. To do so, the electrochemical polarization resistance technique will be used to monitor the corrosion process and determine mass loss, in addition to evaluating the morphology (SEM/EDS) and crystalline phase formation (XRD) of the film formed on the steel surface.

2. Methodology

2.1. Zinc coating deposition

Samples of AISI 1020 steel, measuring 20 mm on each side with a thickness of 2 mm, were used for the experimental procedure. These samples underwent electroplating galvanization before the surface treatment, which involved immersion in a 0.1 M oxalic acid solution. Electroplating was employed for galvanizing the samples, utilizing an electrical circuit to deposit ions from the electrolytic solution onto the steel sample surfaces through the application of electric current. The composition of the solutions used followed the description by[26], according to Table 1.

Table 1. Composition of the electrolytic solution used for zinc electroplating[26].

Compound	Concentration (g/l)	Concentration (mol/l)
Potassium Chloride (KCl)	208.0	2.790
Zinc Chloride (ZnCl)	19.6	0.144
Boric Acid (H_3BO_3)	20.0	0.325

Before galvanization, the samples underwent a cleaning treatment to enhance zinc coating adhesion. This treatment included mechanical grinding with silicon carbide sandpaper to remove oxidation residues, immersion in a sulfuric acid solution [0.5M], additional grinding for surface uniformity, followed by rinsing with distilled water and acetone to remove impurities, and drying with an electric dryer at 80°C for 5 minutes.

The electrical circuit was set up by connecting a power supply (MPS-3035D MINIPA) to a graphite electrode immersed in the electrolytic solution, ensuring uniform distribution of electrical current across the solution and steel samples. Unlike the hot-dip galvanization process, which results in very thick coating layers (over 80 µm), the typical zinc coating obtained by electroplating does not exceed 20 µm in thickness, as per ASTM A767-09:15 standard. For this study, a coating thickness of 5 µm was selected to allow for comparisons and evaluate its effectiveness even with thinner layers. After calculations, it was determined that an applied current of 314.6 mA (current density of 20 mA/cm^2) was needed, with an electroplating time of 9 minutes.

2.2. Surface treatment

After electroplating, the samples were divided into two groups, with only half of them undergoing surface treatment in a 0.1 M oxalic acid solution (Table 2). The treated samples underwent three sequential ultrasonic baths in acetone, ethanol, and water, followed by drying with hot air for 5 seconds. Subsequently, the samples were air-cooled for 2 minutes before immersion in the oxalic acid solution for 5 minutes. After treatment, the samples were air-dried for 5 minutes and then placed in an oven at 90°C for 15 minutes and stored in a desiccator. The treatment solution consisted of 118.5 g $Ca(OH)_2$, 0.9 g NaOH, and 4.2 g KOH per liter of solution. The saline solution simulated an environment composed of [0.5M] NaCl per liter of solution.

2.3. Immersion in corrosive environment

After cleaning, electroplating, and treatment with oxalic acid solution, the test samples were divided into two batches and immersed in an alkaline solution (pH around 13) and a slightly acidic solution (pH around 6.5) for 168 hours. The alkaline solution used simulates the solution present in concrete pores, produced according to ACI 4403R-04 method[27], and composed of 118.5 g $Ca(OH)_2$, 0.9 g NaOH, and 4.2 g KOH per liter of solution. The saline solution simulates an environment composed of [0.5M] NaCl per liter of solution. All experiments were performed in triplicate.

2.4. Surface characterization of steel

The morphology and point chemical composition of the samples were assessed using Scanning Electron Microscopy

Table 2. Composition of the oxalic acid solution used for surface treatment (OLIVEIRA, 2018).

Compound	Concentration (g/l)
Oxalic acid ($H_2C_2O_4$)	0.10
Sodium nitrate ($NaNO_3$)	0.02
Sodium sulfate (Na_2SO_4)	0.02

(SEM) and Energy Dispersive Spectroscopy (EDS). X-ray Diffraction (XRD) was employed to determine the mineralogical composition. These evaluations were conducted before and after immersion in corrosive solutions. Morphological evaluations and point chemical and mineralogical compositions of the galvanized samples were performed before (0h) and after immersion in alkaline solution for 24, 48, 72, 120, and 168 hours.

Scanning Electron Microscopy (SEM) was performed using a VEGA 3 LMU TESCAN microscope, equipped with secondary electron (SE) and backscattered electron (BSE) detectors, as well as Energy Dispersive Spectroscopy (EDS). The SEM operated with an accelerating voltage of 20 kV and a tungsten filament. The samples were analyzed before and after 24, 48, 72, 120, and 168 hours of immersion in an alkaline solution. Additionally, the samples were exposed to a NaCl [0.1M] solution to conduct a comparative study on the influence of pH.

The mineralogical composition was determined through X-Ray Diffraction (XRD), using a D2 Phaser Bruker diffractometer with a copper target tube ($\lambda = 0.15406$ nm), operating at 30 kV and 10 mA. The diffraction spectra were collected in the 2θ range of 5° to 80°, with a step size of 0.004°/s. The phases were identified and quantified using specialized software (DIFFRAC plus - EVA and TOPAS).

2.5. Electrochemical corrosion measurements and mass loss evaluation

To assess polarization resistance, an electrochemical cell was assembled using an Ag/AgCl reference electrode (saturated with KCl) and a platinum wire as the counter electrode, with the central region of the sample serving as the working electrode. Measurements were conducted in an alkaline solution simulating concrete pH, using a Gamry 1010ETM potentiostat with impedance module and Gamry Framework™ software version 7.

The potentiodynamic curves were generated at a scan rate of 10 mV/s and a potential range of ±800 mV around the open circuit potential. The corrosion current density (I_{corr}) and corrosion potential (E_{corr}) were determined from Tafel extrapolation curves, with each coating process analyzed in triplicate.

Additionally, mass loss was evaluated using a gravimetric method to quantify the average corrosion rate over time. Following the NACE-RP-07-75[28] standard, the mass loss of the samples before and after exposure to the corrosive environment was measured. This quantitative analysis enabled the determination of the corrosion rate and, consequently, the evaluation of the treatment's effectiveness in protecting against degradation.

3. Results and Discussions

3.1. Surface treatment of steel samples

3.1.1. Analysis of the effect of conversion treatment on the morphology of zinc deposit through scanning electron microscopy (SEM)

Figure 1 presents scanning electron micrographs of the electrodeposited surfaces in untreated samples (Figure 1A) and samples treated in oxalic acid solution (Figure 1B).

While the untreated samples exhibit a surface composed of irregular and elongated particles, the treated samples reveal a more porous morphology with prismatic particles, indicating the formation of a zinc oxalate layer. This layer promotes early formation of corrosion products, increasing corrosion resistance.

Figures 2 and 3 show the scanning electron micrographs of the electrodeposited surfaces of untreated samples (Figure 2) and samples treated with oxalic acid solution (Figure 3) after different immersion periods in the NaCl solution [0.1M].

Up to 168 hours of immersion in the corrosive medium, no significant changes were observed in the morphology of the surface of the samples untreated with oxalic acid (Figure 2). The formed grains exhibit irregular shapes and dimensions, and over time, a small reduction in grain size is observed. In the samples treated with oxalic acid, significant changes in morphology were observed, with changes in grain dimensions and shapes, as well as a higher degree of compaction (Figure 3).

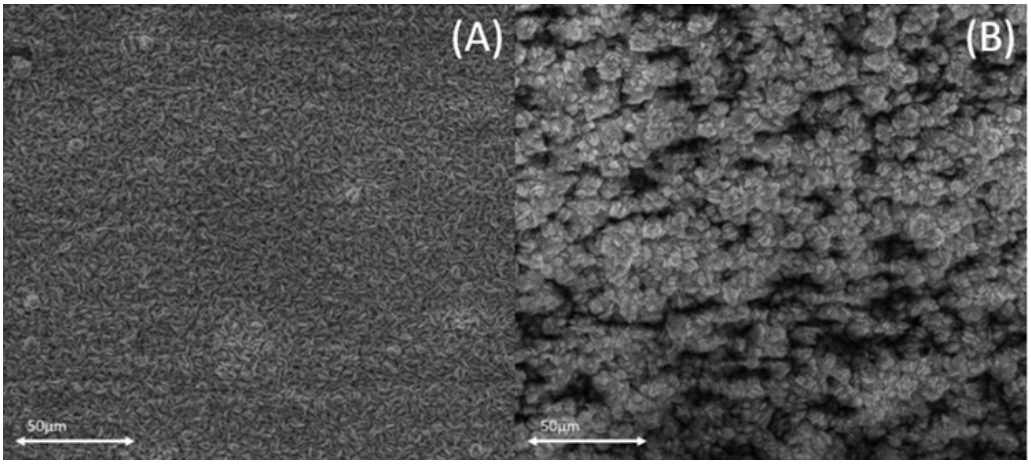

Figure 1. Micrographs of the electrodeposited surfaces: (a) untreated and (b) treated in 0.1 M oxalic acid solution, before exposure to the alkaline solution.

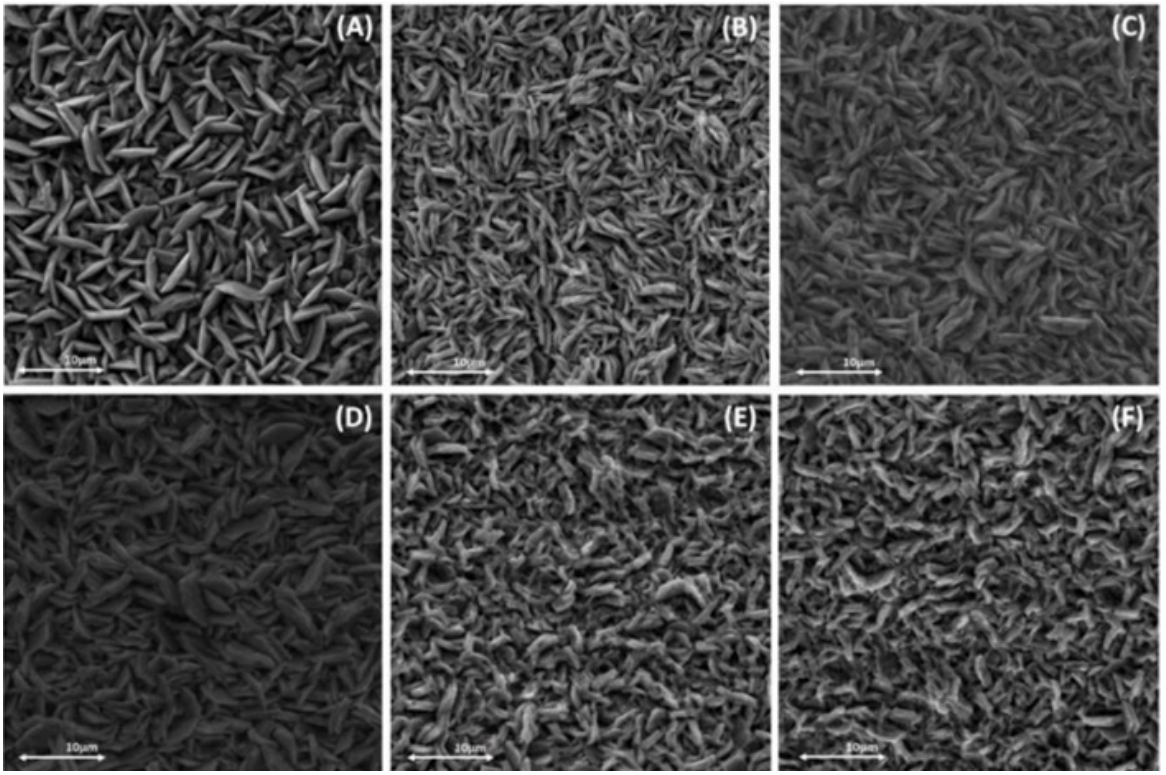

Figure 2. Micrographs of untreated electrodeposited surfaces in solution with oxalic acid, (a) before and after (b) 24 hours, (c) 48 hours, (d) 72 hours, (e) 120 hours, and (f) 168 hours of immersion in NaCl solution [0.1M].

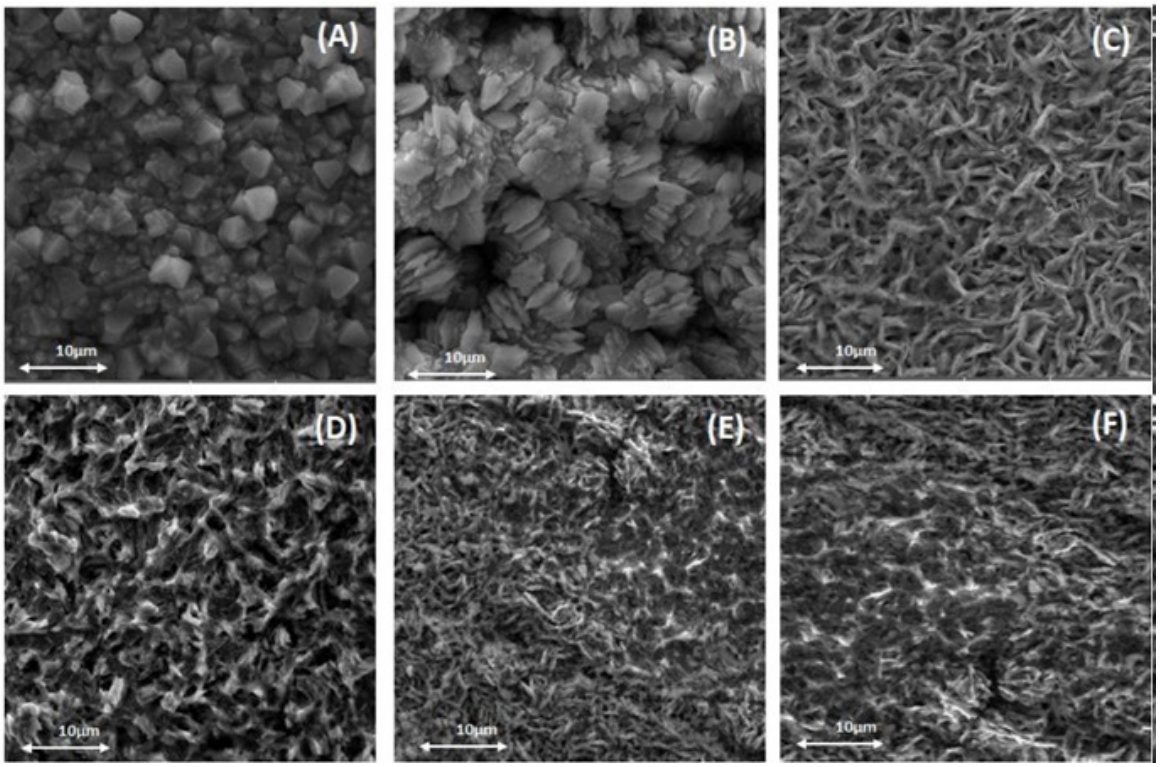

Figure 3. Micrographs of electrodeposited surfaces treated in solution with oxalic acid, (a) before and after (b) 24 hours, (c) 48 hours, (d) 72 hours, (e) 120 hours, and (f) 168 hours of immersion in NaCl solution [0.1M].

As previously described, samples subjected to treatment with oxalic acid exhibit more porous and irregular surfaces, which can lead to corrosive attack on the metallic substrate. In Figure 3B, it is possible to observe that, with only 24 hours of immersion in the corrosive medium, a significant portion of the zinc oxalate coating was removed. The removal of part of this coating promoted greater contact of the surface with the corrosive medium and, consequently, the formation of corrosion products that remain adhered to the substrate.

According to[21], from the early moments of contact with the corrosive solution, the porosity of the oxalate layer allows the infiltration of the sodium chloride solution and the formation of the first zinc corrosion products, which apparently grow from the substrate to the surface through the oxalate coating. The formation of these corrosion products may be related to the formation of a more uniform deposit after longer immersion times, as can be observed in Figures 3D, 3E, and 3F.

Table 3 presents the elemental contents detected by EDS on the electrodeposited surfaces, with and without treatment in oxalic acid solution, before and after 24, 48, 72, 120, and 168 hours of immersion in NaCl solution [0.1M].

Based on the results presented in Table 3, untreated samples show a surface layer primarily composed of zinc, indicating galvanized steel, with a small concentration of iron, the substrate's most abundant element, associated with film defects caused by the low coating thickness. In contrast, samples treated with oxalic acid exhibit significantly lower zinc concentration and higher levels of carbon and oxygen, suggesting the presence of zinc oxalate, a product of zinc and oxalic acid interaction. Zinc coating protects steel primarily through a mechanical barrier. When coating defects occur (such as porosity or scratches), protection shifts to sacrificial corrosion of the zinc layer. Micrographs of treated and untreated samples reveal coating defects and porosity. Elemental mappings confirm iron presence, indicating these defects.

Morphological changes in acid-treated samples suggest the presence of zinc corrosion products, potentially enhancing corrosion resistance. Both sample types exhibit reduced zinc and increased iron concentrations after 120 hours of corrosive exposure, indicating coating degradation. Zinc's protective efficacy depends heavily on coating durability against corrosion, influenced by coating thickness and environmental conditions. Increased iron concentration suggests coating removal, indicating the need for thicker coatings over longer exposure periods.

Figure 4 shows the scanning electron micrographs corresponding to the electrodeposited surfaces of samples that were not treated in oxalic acid solution after different immersion periods in an alkaline solution similar to that observed in concrete pores.

Figure 5 shows the scanning electron micrographs corresponding to the electrodeposited surfaces of samples treated in oxalic acid solution after different immersion periods in an alkaline solution similar to that found in concrete pores.

The micrographs of the untreated samples (Figure 4B) and treated samples (Figure 5B) show significant changes in surface morphology after a short period of immersion in an alkaline solution. The dissolution of the zinc oxalate coating promotes a more irregular and porous surface, intensifying the corrosion process.

Table 4 presents the surface elemental compositions of the electrodeposited bars, both untreated and treated in oxalic acid solution, before (0h) and after 24, 48, 72, 120, and 168 hours of immersion in an alkaline solution, as obtained by EDS.

Energy Dispersive Spectroscopy (EDS) analyses revealed changes in the concentration of surface elements after immersion in an alkaline solution. Samples treated with oxalic acid showed a more pronounced decrease in oxygen and carbon concentrations, indicating the dissolution of the oxalate layer and exposure of the substrate to the corrosive environment.

A higher concentration of iron was observed on the electrodeposited surfaces of both untreated and treated samples in oxalic acid solution, indicating the removal of the coating and exposure of the substrate. The chemical analysis of the samples revealed variations in surface composition over the immersion period, highlighting the formation of corrosion products such as calcium zinc hydroxide, which acts as a protective film.

These results suggest that the effectiveness of the conversion treatment in corrosion protection is related to the porosity of the zinc oxalate layer, which influences the rate of dissolution and formation of corrosion products. Understanding these processes is essential for developing more effective and durable protection strategies for metallic structures.

Table 3. Contents of elements detected by EDS on electrodeposited surfaces, with and without treatment in oxalic acid solution, before (0h) and after 24, 48, 72, 120, and 168 hours of immersion in NaCl solution [0.1M].

Exposure Time	Untreated Samples				Treated Samples			
	Detected Contents (%, by mass)				Detected Contents (%, by mass)			
	Zn	Fe	O	C	Zn	Fe	O	C
0h	97.26	2.74	-	-	31.56	0.54	52.48	16.43
24h	96.02	1.53	1.03	-	66.14	1.31	24.88	7.56
48h	95.29	1.30	2.10	-	92.59	2.21	2.97	2.24
72h	96.55	1.38	1.02	-	91.79	1.87	3.97	2.37
120h	88.35	10.95	2.71	-	80.14	15.21	3.11	1.54
168h	83.52	13.66	2.82	-	79.15	16.53	3.12	1.20

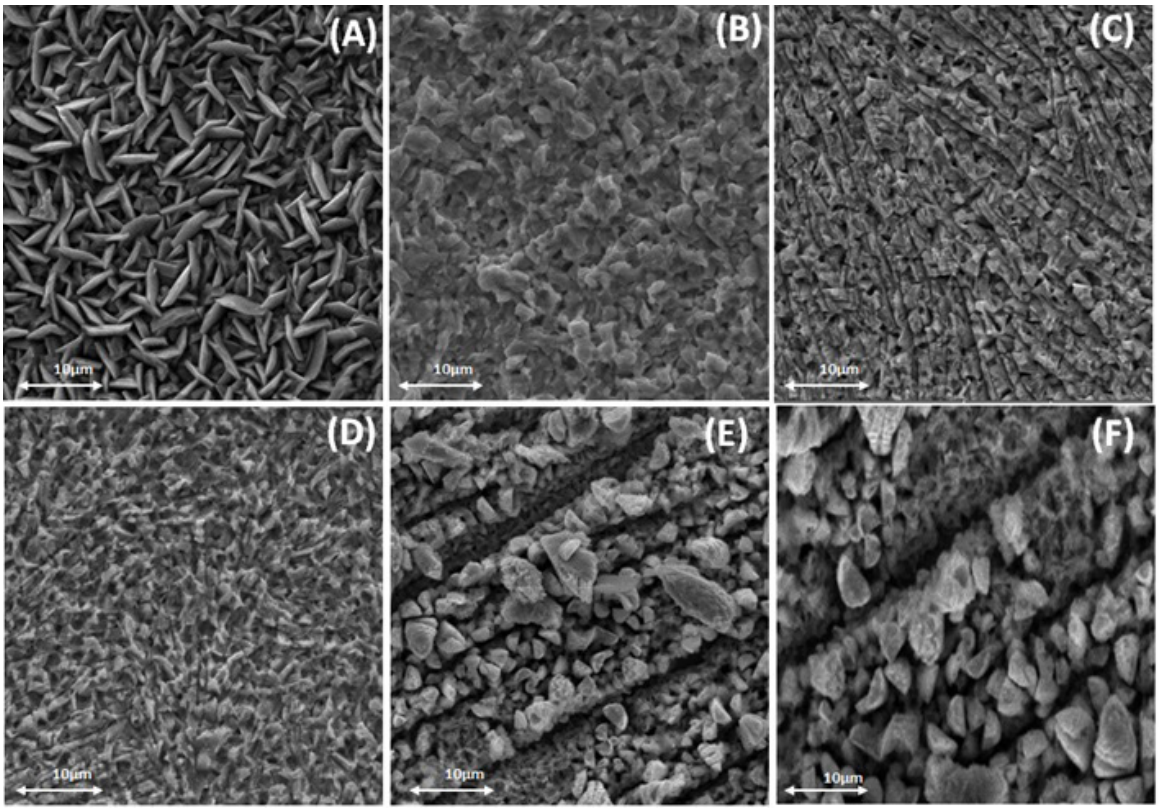

Figure 4. Micrographs of untreated electrodeposited surfaces in solution with oxalic acid, (a) before and after (b) 24 hours, (c) 48 hours, (d) 72 hours, (e) 120 hours, and (f) 168 hours of immersion in in alkaline solution.

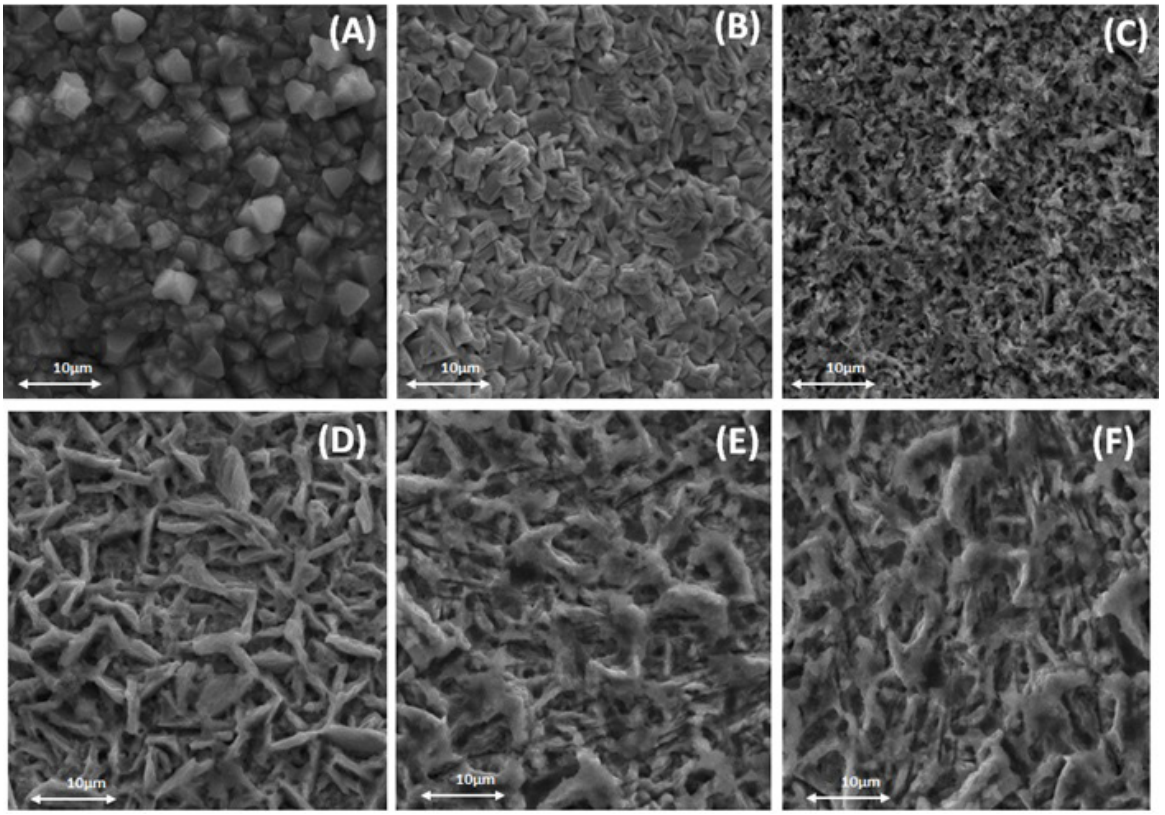

Figure 5. Micrographs of electrodeposited surfaces treated in solution with oxalic acid, (a) before and after (b) 24 hours, (c) 48 hours, (d) 72 hours, (e) 120 hours, and (f) 168 hours of immersion in alkaline solution.

Table 4. Surface elemental compositions of the electrodeposited bars, both untreated and treated in oxalic acid solution, before (0h) and after 24, 48, 72, 120, and 168 hours of immersion in an alkaline solution, as obtained by EDS.

Exposure Time	Untreated Samples				Treated Samples				
	Detected Contents (%, by mass)				Detected Contents (%, by mass)				
	Zn	Fe	O	C	Zn	Fe	O	C	Ca
0h	97.26	2.74	-	-	51.61	2.22	8.13	38.04	-
24h	93.39	6.61	-	-	92.69	2.65	1.46	3.66	-
48h	96.24	3.76	-	-	90.94	5.44	1.51	2.11	-
72h	95.59	441	-	-	97.29	2.71	-	-	-
120h	91.14	6.21	0.76	1.89	89.04	1.04	1.90	7.56	0.37
168h	90.51	7.64	0.55	1.56	88.21	3.78	1.89	1.89	0.47

3.1.2. Analysis of the influence of surface treatment on the formation of crystalline phases

Figure 6 presents the diffractograms of the electroplated samples with and without treatment in oxalic acid solution [0.1M], before exposure to alkaline solution for 24 hours. Peaks associated with the crystalline phases of zinc (Z) and iron (F) are identified. The identification of crystalline phases of iron is evidence that the deposited surface did not exhibit the desired uniformity, indicating that the coating thickness was insufficient, as observed in the micrographs (SEM) and elemental maps (EDS).

It can be observed the formation of characteristic peaks of hydrated zinc oxalate ($ZnC_2O_4.2H_2O$) in the diffractogram of the sample treated in oxalic acid solution [0.1M] before exposure to alkaline solution and NaCl solution [0.1M], indicating the deposition of the product on the surface of the steel substrate. The existence of this layer is associated with an early increase in the corrosion resistance of the parts.

Figures 7A to 11 present the diffractograms of the surfaces of the electroplated samples that were not treated in oxalic acid solution, after 24, 48, 72, 120, and 168 hours of immersion in NaCl solution [0.1M] and (B) exposure to the alkaline solution.

After 24 hours of immersion (Figure 8A), diffractograms show peaks corresponding to zinc (Z), iron (F), and zinc oxalate layer (O), similar to those observed before exposure to alkaline solution. Subsequent 48-hour immersion (Figure 9A) reveals additional peaks related to zinc oxide (ZnO - Zo), zinc (Z), iron (F), and zinc oxalate layer (O). By 72 hours (Figure 9A), there's a noticeable decrease in zinc oxalate peak intensity, indicating gradual dissolution over time in the corrosive environment.

Zinc oxide (ZnO) is exclusively found in coatings from alkaline baths and can alter the composition and solubility of corrosion products, potentially reducing corrosion rates within the coatings. Its formation can deplete metallic zinc, described by Equation 1[20]:

$$Zn_{(s)} + O_{2(g)} \rightarrow ZnO_{(s)} \quad (1)$$

Figures 10A and 11A depict diffractograms of electroplated samples, with and without oxalic acid treatment [0.1M], after exposure to NaCl solution for 72 and 120 hours, respectively. Untreated samples show initial zinc oxide peaks after 120 hours, while treated samples exhibit consumption of the zinc oxalate layer and emergence of simonkolleite [$Zn_5(OH)Cl_2.8H_2O$] and zinc hydroxide [$Zn(OH)_2$].

In scenarios where zinc coatings exhibit flaws or porosity, zinc functions as an anode (Equation 2)[20], with the exposed steel surface behaving as a cathode (Equation 3)[20]. This cathodic protection mechanism results in the formation of zinc hydroxide (Equation 4)[20] in samples treated with oxalic acid:

$$Zn \rightarrow Zn^{2+} + 2e^- \quad (2)$$

$$H_2O + \frac{1}{2}O_2 + 2e^- \rightarrow 2OH^- \quad (3)$$

$$Zn^{2+} + OH^- \rightarrow Zn(OH)_2 \quad (4)$$

Formation of zinc hydroxide in oxalic acid-treated samples indicates that porosity created by the zinc oxalate layer accelerates zinc corrosion product formation, which can be protective. This is further supported by early simonkolleite presence in untreated samples.

Applying an organic coating like oxalic acid can effectively delay simonkolleite formation, a major corrosion product in chloride-rich environments, thereby enhancing corrosion resistance[20,29]. In conditions of prolonged zinc surface exposure to high humidity, zinc hydroxide forms, which, in the presence of CO2 during drying and wetting cycles, converts into zinc hydroxide carbonate (Equation 5)[20].

$$Zn(OH)_{2(S)} + 4Zn^{+2} + 4OH^- + 2CO_3^{-2} \rightarrow Zn_5(CO_3)_2(OH)_6 \quad (5)$$

Zinc hydroxide carbonate, a metastable compound, in the presence of water and chlorides, forms zinc chlorohydroxysulfate [$NaZn_4Cl(OH)_6SO_4.6H_2O$] and simonkolleite. In chloride-free water environments, only zinc hydroxide carbonate forms. Simonkolleite, a basic chloride, sparingly soluble in water, persists in corrosion product layers formed in acidic and neutral environments, particularly in marine atmospheres, influencing short and long-term corrosion resistance[29].

In the diffractograms of electroplated samples with and without oxalic acid treatment [0.1M], before (Figure 7) and after (Figure 8B) exposure to alkaline solution for 24 hours, only peaks corresponding to zinc (Z) and iron (F) crystalline phases are visible. Hydrated zinc oxalate ($ZnC_2O_4.2H_2O$) appears solely in the sample treated with oxalic acid before exposure (Figure 7i), indicating its deposition on the zinc-plated surface and contributing to early corrosion resistance. However, after 24 hours in alkaline solution, hydrated zinc oxalate peaks disappear (Figure 8Bi), signifying its dissolution.

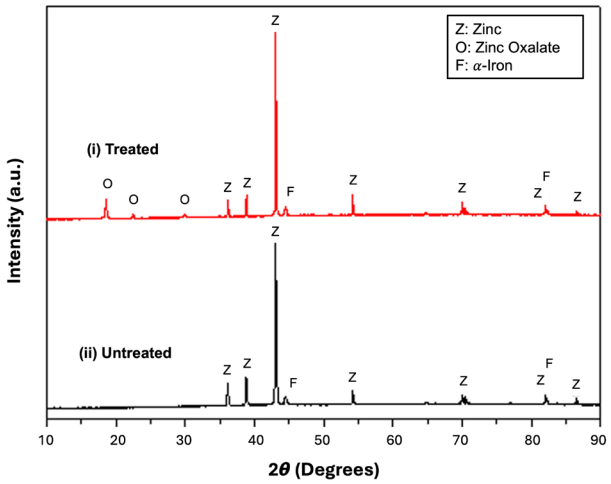

Figure 6. Diffractograms of the surfaces of electrodeposited samples (i) with and (ii) without treatment in oxalic acid solution [0.1M], before exposure to alkaline solution and NaCl solution [0.1M] (0h).

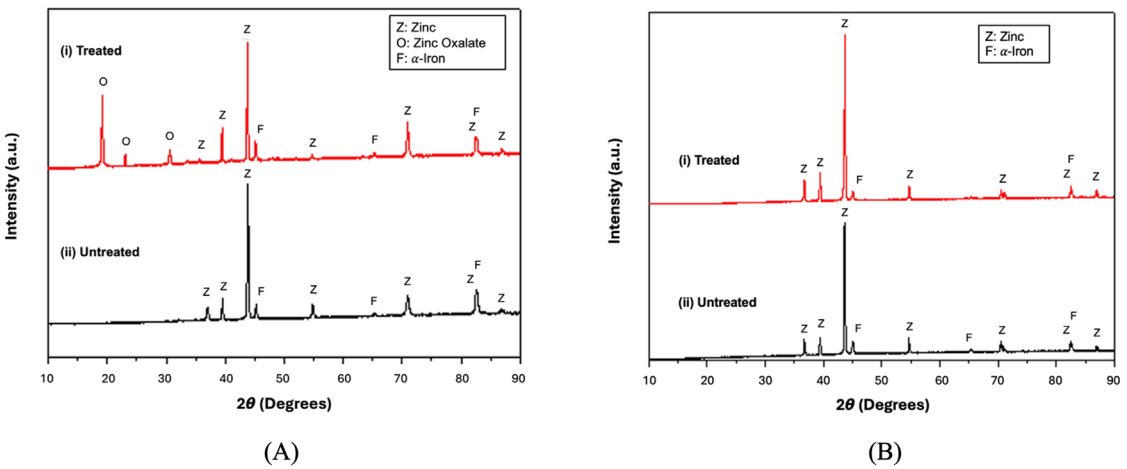

(A) (B)

Figure 7. Diffractograms of the surfaces of electrodeposited samples (i) with and (ii) without treatment in oxalic acid solution [0.1M], after 24h of immersion in (A) NaCl solution [0.1M] and (B) exposure to the alkaline solution.

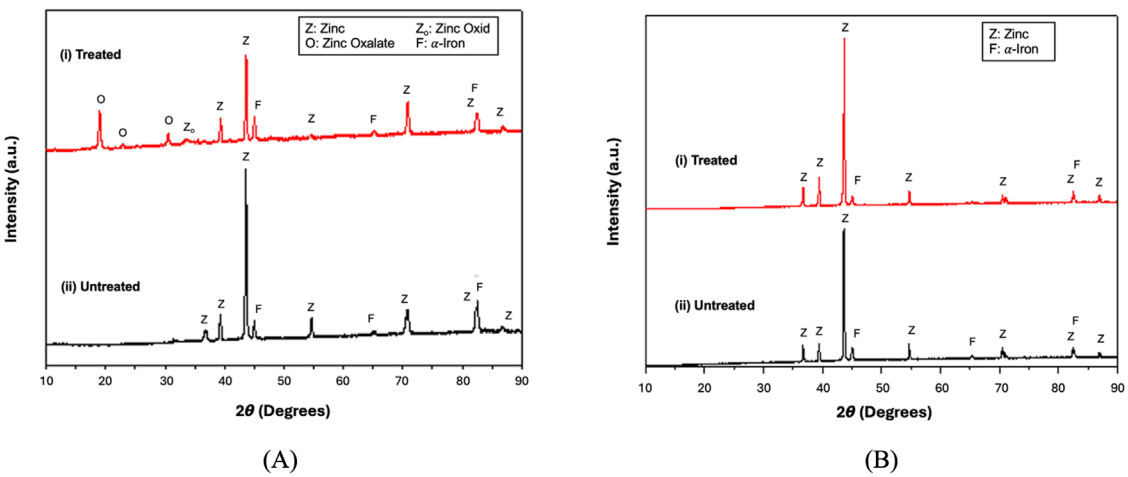

(A) (B)

Figure 8. Diffractograms of the surfaces of electrodeposited samples (i) with and (ii) without treatment in oxalic acid solution [0.1M], after 48 hours of immersion in (A) NaCl solution [0.1M] and (B) exposure to the alkaline solution.

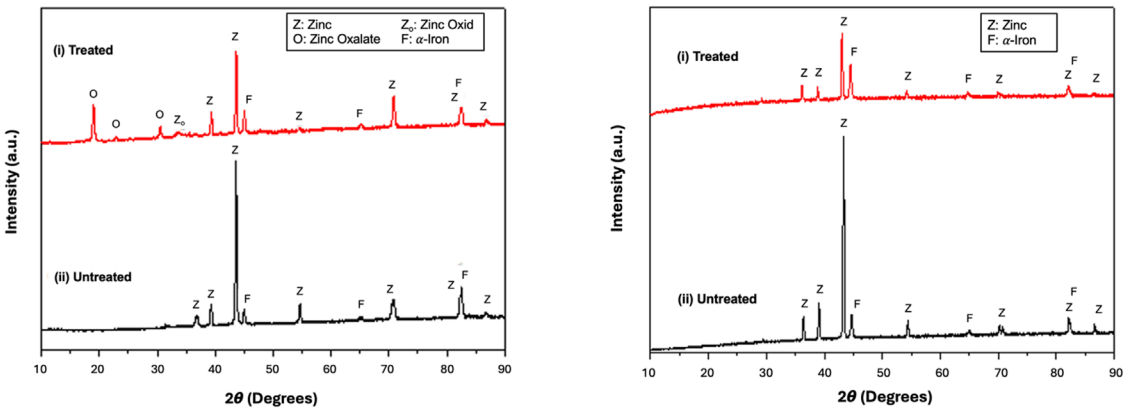

Figure 9. Diffractograms of the surfaces of electrodeposited samples (i) with and (ii) without treatment in oxalic acid solution [0.1M], after 72 hours of immersion in (A) NaCl solution [0.1M] and (B) exposure to the alkaline solution.

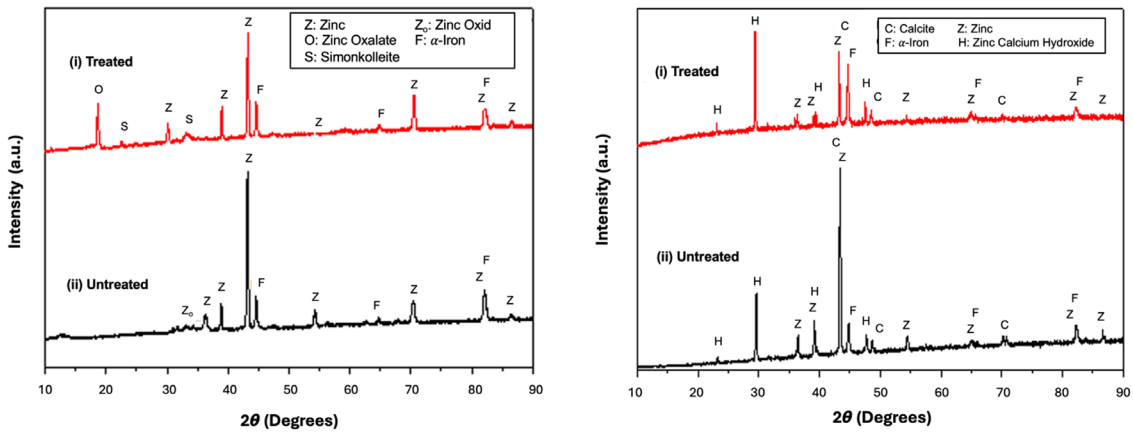

Figure 10. Diffractograms of the surfaces of electrodeposited samples (i) with and (ii) without treatment in oxalic acid solution [0.1M], after 120 hours of immersion in (A) NaCl solution [0.1M] and (B) exposure to the alkaline solution.

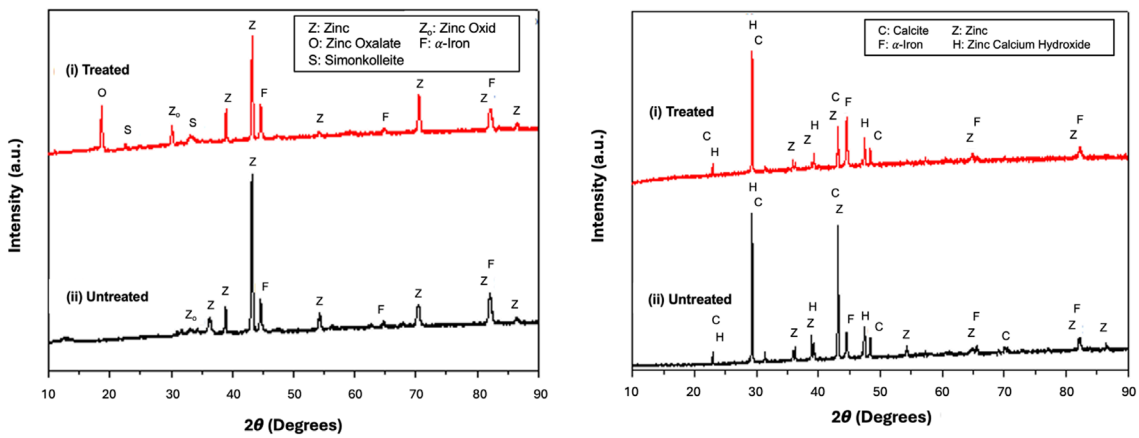

Figure 11. Diffractograms of the surfaces of electrodeposited samples (i) with and (ii) without treatment in oxalic acid solution [0.1M], after 168 hours of immersion in (A) NaCl solution [0.1M] and (B) exposure to the alkaline solution.

Untreated samples (Figure 7ii) show no changes after exposure to alkaline solution, similar to their pre-exposure state. Samples immersed for 48 hours (Figure 9B) exhibit no significant changes, indicating stability in alkaline conditions over this period.

After 72 hours in alkaline solution (Figure 10Bi), treated samples show reduced peak intensities of zinc crystalline phases (2θ at 36.3°, 39.0°, 43.3°, 54.6°, and 70.7°), suggesting formation of zinc-containing corrosion products. Elemental mapping by EDS (Table 4) confirms presence of only Zn and Fe between 48 and 72 hours, indicating minimal zinc compound formation.

After 120 hours (Figure 11B), both treated and untreated samples exhibit calcite ($CaCO_3$, C) and calcium zinc hydroxide ($Ca[Zn(OH)_3]_2.2H_2O$, H) formation. Surface mapping (Table 4) identifies oxygen, carbon, and calcium elements, consistent with morphological changes induced by these compounds.

Calcium zinc hydroxide, a primary zinc corrosion product in alkaline solutions, forms a protective passive film, enhancing corrosion resistance of galvanized steel[30]. Its formation is described by equations 6 and 7[31]:

$$Zn + 2H_2O \rightarrow Zn(OH)_2 + H_2 \quad (6)$$

$$2Zn(OH)_2 + 2H_2O + Ca(OH)_2 \rightarrow Ca[ZnOH_3]_2.2H_2O \quad (7)$$

This film's effectiveness in enhancing corrosion resistance depends on the alkaline environment's pH, typically optimal between 12.0 and 12.8[32]. Above pH 13.3 ± 0.1, zinc can become active, potentially initiating corrosion. In contrast to samples in NaCl [0.1M] solution, where zinc oxide and zinc hydroxide enhance corrosion resistance, these products were not identified on surfaces exposed to alkaline environments

3.2. Evaluation of corrosion resistance

3.2.1. Evaluation of mass loss (gravimetric method)

The mass losses observed in the plates immersed in alkaline medium (Table 5) and in solution containing NaCl (Table 6) allowed estimating the average corrosion rates and classifying them according to the criteria for assessing corrosiveness described in the NACE RP-07-75 standard[28]. The development of corrosion rates as a function of immersion time in the studied solutions is presented in Figure 12.

Treatment with oxalic acid [0.1M] significantly enhanced corrosion resistance in samples exposed to NaCl [0.1M] solutions over 168 hours (Figure 12 and Table 6). This effect was attributed to early formation of zinc corrosion products like zinc oxide, zinc hydroxide, and simonkolleite. Passivation of zinc occurred due to the zinc oxalate layer formed after oxalic acid treatment, its effectiveness influenced by oxalic acid concentration and layer thickness.

Scanning Electron Microscopy (SEM) micrographs revealed notable differences in the morphology of the surfaces of treated and untreated samples. Untreated samples (Figure 1A) exhibited irregular and elongated particles, while treated samples (Figure 1B) displayed a more porous morphology characterized by the presence of prismatic particles. This change in microstructure indicates the formation of a zinc oxalate layer, which, according to the literature, enhances corrosion resistance.

The EDS analysis showed that treated samples had a reduced concentration of zinc compared to untreated samples, suggesting that the zinc oxalate layer was dissolving, contributing to the higher corrosion rates observed in these samples. The presence of corrosion products, such as zinc hydroxide formed in response to accelerated zinc corrosion, was confirmed by X-ray diffraction (Figure 6). The diffractograms showed characteristic peaks of hydrated zinc oxalate in treated samples, indicating the formation of a layer that should, in principle, provide protection.

As immersion times increased, treated samples exhibited a marked decrease in the intensity of the zinc oxalate peaks in the diffractograms, indicating that the dissolution of this layer was accompanied by an increase in the formation of corrosion products, which was directly related to the rising corrosion rates. Therefore, the correlation between surface morphology, EDS data, and corrosion rates suggests that the efficacy of the conversion treatment in corrosion protection is closely linked to the porosity of the zinc oxalate layer and its ability to resist dissolution in corrosive environments.

Table 5. Corrosion rates (mm/year) of samples without and with treatment in oxalic acid solution [0.1M], immersed in alkaline solution, over time.

Parameter	Immersion time in alkaline solution				
	24h	48h	72h	120h	168h
Corrosion rate in untreated samples (mm/year)	0.2243 ± 0.0913 (high)	0.4652 ± 0.0318 (severe)	0.4776 ± 0.2659 (severe)	0.4338 ± 0.0519 (severe)	0.2785 ± 0.0333 (severe)
Corrosion rate in treated samples (mm/year)	1.2892 ± 0.1174 (severe)	1.1068 ± 0.2420 (severe)	1.0718 ± 0.0519 (severe)	0.6558 ± 0.0552 (severe)	1.3058 ± 0.36655 (severe)

Table 6. Corrosion rates (mm/year) of samples without and with treatment in oxalic acid solution [0.1M], immersed in NaCl solution [0.1M], over time.

Parameter	Immersion time in alkaline solution				
	24h	48h	72h	120h	168h
Corrosion rate in untreated samples (mm/year)	0.5996 ± 0.0126 (severe)	0.2952 ± 0.0111 (severe)	0.0992 ± 0.0078 (moderate)	0.3268 ± 0.0155 (severe)	0.1978 ± 0.008 (high)
Corrosion rate in treated samples (mm/year)	0.3503 ± 0.0558 (severe)	0.1559 ± 0.0176 (high)	0.0845 ± 0.0072 (moderate)	0.2214 ± 0.0544 (high)	0.1487 ± 0.0530 (high)

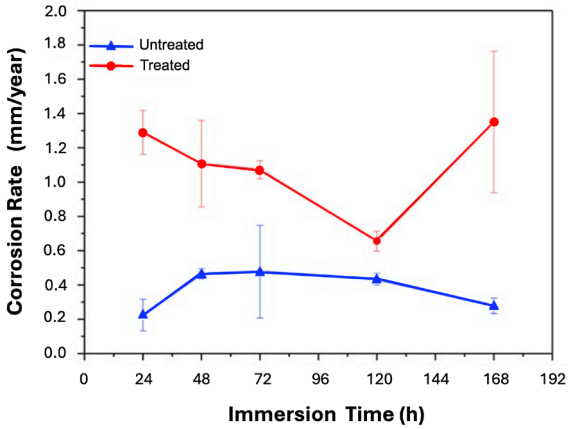

Figure 12. Corrosion rates (mm/year) of samples without and with treatment in oxalic acid solution [0.1M], immersed in NaCl [0.1M] and alkaline solutions, over time.

Furthermore, the analysis of tests in alkaline solutions showed that both treated and untreated samples presented variations in surface composition over time, with an increase in iron concentration indicating the removal of the zinc coating. The corresponding micrographs (Figures 4 and 5) showed significant morphological changes, with more irregular and porous surfaces after immersion, which was directly related to the increased corrosion rates observed in gravimetric measurements.

For immersion periods beyond 72 hours, formation of calcium hydrozincate was observed (Figure 9B), consistent with findings by other researchers[30,31,33,34]. This compound acts as a protective film in alkaline solutions (pH 12.6-13.3), reducing corrosion rates in galvanized steel [34]. Diffractograms (Figures 9B to 11B) confirmed $Ca[Zn(OH)_3]_2.2H_2O$ formation after 72 hours in alkaline solution, further reducing corrosion rates (Tables 5 and 6). According to these authors, the formation of $Ca[Zn(OH)_3]_2.2H_2O$ crystals in pH 12.5 ± 0.1 to 13.3 ± 0.1 solutions (similar to pH 13 in this study) compact the entire zinc surface, promoting passive corrosion.

The trend of decreasing corrosion rate in untreated samples after 120 hours can be explained by the formation of protective corrosion products on the surface of the galvanized steel. In the initial exposure to the corrosive medium (0.1M NaCl solution), the zinc coating undergoes sacrificial corrosion, protecting the underlying steel substrate. As the exposure time increases, corrosion products such as zinc hydroxide ($Zn(OH)_2$) and zinc oxalate begin to form.

The gradual development of these protective layers is directly linked to the reduction in the steel's exposure to the corrosive medium, explaining the observed decrease in corrosion rates after 120 hours. Simultaneously, zinc loss in the samples decreases as these layers become thicker and more stable, resulting in the trend of decreasing corrosion rates over time.

3.2.2. Potentiodynamic Tests

The Tafel polarization curves obtained from the electrodeposited samples with and without treatment in oxalic acid [0.1 M] and exposed to alkaline solution and solution containing NaCl for 24, 48, 72, 120, and 168 hours are presented in Figure 13.

It is observed that, in the anodic region, for the same potential, the current density observed in the samples treated in oxalic acid solution [0.1M] is lower, indicating greater resistance to corrosion, which is consistent with the results presented in Table 7 and with the obtained diffractograms (Figures 6 to 11). Several authors[19-22] highlight oxalic acid as a good alternative to replace chromium and economically viable option for increasing the corrosion resistance of metallic substrates.

Through the micrograph in Figure 2B, it is possible to observe that the surface of the electrodeposited sample undergoes significant changes in its morphology after being subjected to treatment in oxalic acid solution [0.1M]. This occurs due to the formation of the zinc oxalate layer, which is mainly composed of prismatic particles[21,35]. The existence of this more porous surface may be associated with the increase in corrosion resistance, as it facilitates the penetration of the solution and the early formation of the first zinc corrosion products. Zinc oxides and hydroxides develop on the substrate and towards the surface through the oxalate coating, providing increased corrosion resistance[20,21]. For immersion times exceeding 120 hours, the increase in corrosion resistance occurs through the early appearance of simonkolleite, which is the main corrosion product in environments where chlorides are present[21,29].

The corrosion current density (I_{corr}) and the corrosion potential (E_{corr}) of the electrodeposited samples with and without treatment in oxalic acid solution [0.1 M] and exposed to alkaline solution were obtained from the extrapolation of the Tafel curves (Figure 14), as shown in the results presented in Table 8, which represent an average of three determinations.

It is observed that, in the anodic region, for the same potential, the current density observed in the samples untreated in oxalic acid solution [0.1M] is lower, indicating greater resistance to corrosion, which is in accordance with the results presented in Table 8 and with the obtained diffractograms (Figures 6 to 11). This result shows that crystallographic orientation can influence corrosion behavior, since crystal planes of high density would exhibit relatively superior corrosion resistance[36].

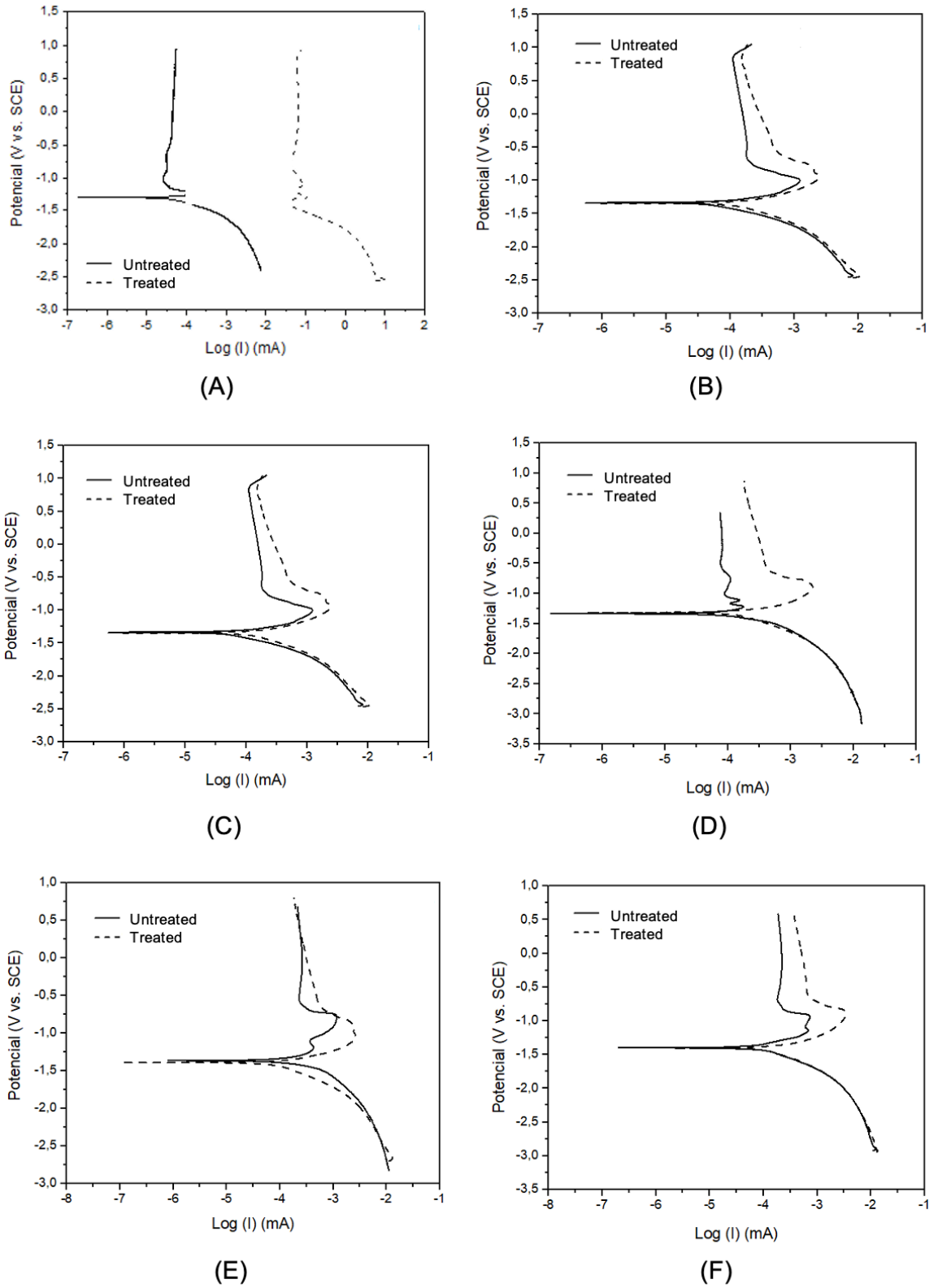

Figure 13. Tafel polarization curves of electrodeposited samples without and with treatment in oxalic acid solution [0.1M], before (a) and after (b) 24 hours, (c) 48 hours, (d) 72 hours, (e) 120 hours, and (f) 168 hours of immersion in alkaline solution.

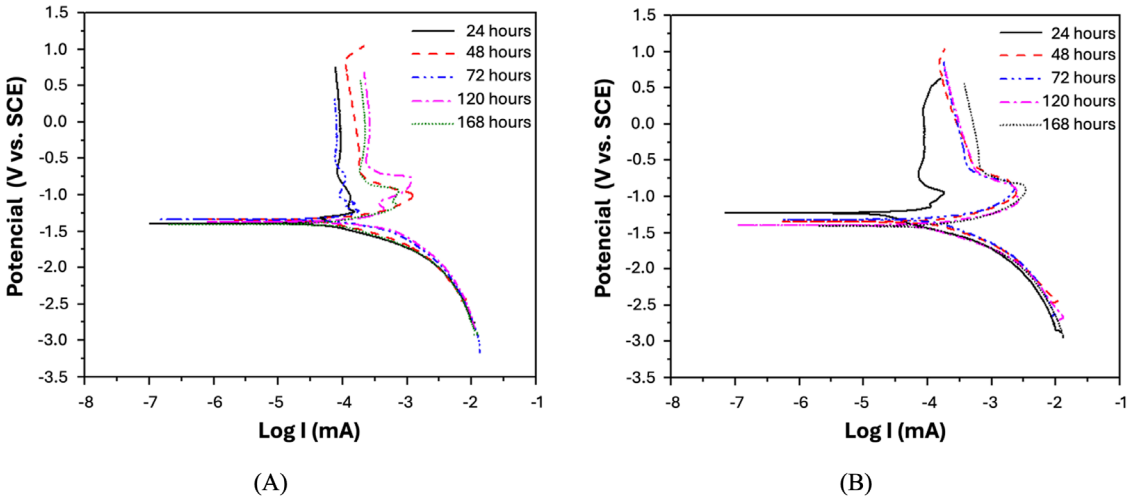

Figure 14. Evolution of Tafel polarization curves of electrodeposited samples without (a) and with (b) treatment in oxalic acid solution [0.1M] during the immersion time in alkaline solution.

Table 7. Values of potential (E_{corr}), current (I_{corr}), and corrosion rates of untreated electrodeposited samples in oxalic acid solution [0.1M], before (0h) and after 24, 48, 72, 120, and 168 hours of immersion in alkaline solution.

Exposure Time	E_{corr} (mV)	I_{corr} (μA)	Corrosion Rate (mm/year)
0h	-1304.24 ± 2.19	-0.035 ± 0.002	5.26 x 10^{-4}
24h	-1347.21 ± 13.44	0.033 ± 0.002	4.94 x 10^{-4}
48h	-1398.45 ± 0.21	0.077 ± 0.007	1.15 x 10^{-3}
72h	-1334.85 ± 1.03	0.089 ± 0.003	1.33 x 10^{-3}
120h	-1368.58 ± 8.69	0.213 ± 0.008	3.20 x 10^{-3}
168h	-1379.38 ± 3.11	0.073 ± 0.050	1.08 x 10^{-3}

Table 8. Values of potential (Ecorr), current (Icorr), and corrosion rates of electrodeposited samples treated in oxalic acid solution [0.1M], before (0h) and after 24, 48, 72, 120, and 168 hours of immersion in alkaline solution.

Exposure Time	E_{corr} (mV)	I_{corr} (μA)	Corrosion Rate (mm/year)
0h	-1390.87 ± 0.02	30.500 ±1.005	4.70 x 10^{-1}
24h	-1364.88 ± 13.99	0.051 ± 0.016	7.64 x 10^{-4}
48h	0.13 ± 0.01	0.127 ± 0.005	1.90 x 10^{-3}
72h	-1357.78 ± 0.71	0.154 ± 0.005	2.31 x 10^{-3}
120h	-1424.30 ± 0.64	0.095 ± 0.043	1.42 x 10^{-3}
168h	-1449.69 ± 2.12	0.134 ± 0.007	2.01 x 10^{-3}

It is observed in Figure 14 and in Tables 7 and 8 that immersion of the samples treated in oxalic acid solution [0.1M] increases the corrosion current density (I_{corr}), and consequently, the corrosion rate in samples immersed in alkaline solution, especially after 120 hours of immersion, reducing the corrosion potential (E_{corr}). The lower the value of E_{corr}, the lower the chloride content needed to trigger the corrosive process, that is, the critical chloride content ($\%Cl^-_{crit}$).

As observed in the diffractograms displayed in Figures 10B and 11B, $Ca[Zn(OH)_3]_2.2H_2O$ is formed in samples immersed in alkaline solution for 120 and 168 hours. As a consequence of these observations, lower corrosion rates can be expected if the interaction between the concrete matrix and galvanized reinforcements produces a compact and continuous layer of $Ca[Zn(OH)_3]_2.2H_2O$ on the zinc coatings. In the presence of a discontinuous layer of $Ca[Zn(OH)_3]_2.2H_2O$ and/or $Zn(OH)_2$ and ZnO, corrosion rates can be significantly high[30,33,34].

According to Román et al.[37], the non-uniform distribution of this corrosion product on galvanized steel can cause heterogeneous access of chlorides to the rebar, resulting in localized corrosion and, consequently, compromising the structural integrity of the components. Therefore, the proper formation and distribution of $Ca[Zn(OH)_3]_2.2H_2O$ are essential

to ensure effective protection against corrosion in aggressive environments, such as those found in reinforced concrete structures. Understanding these corrosion processes and the influence of surface treatments is crucial for the development of more effective and long-lasting protection strategies for metal structures exposed to corrosive environments.

4. Conclusion

The research demonstrates that the formation of zinc oxalate is essential for the corrosion protection of galvanized steel, acting as a passive film that significantly reduces the corrosion rate after immersion in a 0.1 M oxalic acid solution. However, treatment with oxalic acid did not yield the expected results, leading to an increased corrosion rate, possibly due to the dissolution of zinc oxalate and the formation of a less uniform layer of calcium zinc hydroxide.

It was observed that corrosion resistance varies with immersion time in alkaline solution, with untreated samples showing improved resistance after 168 hours, while those treated with oxalic acid exhibited an initial increase followed by a decrease.

Finally, the research underscores the importance of evaluating the corrosion resistance of galvanized steel bars in contact with concrete, taking into account specific environmental characteristics such as concrete composition and the ionic activity of solutions within the pores, to determine the effectiveness of treatments involving oxalic acid.

5. References

1. Al-Saleh SA. Analysis of total chloride content in concrete. Case Studies in Construction Materials. 2015;3:78-82. http://doi.org/10.1016/j.cscm.2015.06.001.
2. Meira GR. Corrosão de armaduras em estruturas de concreto: fundamentos, diagnóstico e prevenção. João Pessoa: IFPB; 2017.
3. Kumar V. Protection of steel reinforcement for concrete: a review. Corros Rev. 1998;16(4):317-58. http://doi.org/10.1515/CORRREV.1998.16.4.317.
4. Smith JL, Virmani YP. Materials and methods for corrosion control of reinforced and prestressed concrete structures in new construction. United States: Federal Highway Administration; 2000. https://doi.org/10.1088/1757-899X/1114/1/012006
5. Bertolini L. Steel corrosion and service life of reinforced concrete structures. Struct Infrastruct Eng. 2008;4(2):123-37. http://doi.org/10.1080/15732470601155490.
6. Patel R. Prevention of corrosion of steel reinforcement in concrete. AIP Conf Proc. 2019;2158(1):020035. http://doi.org/10.1063/1.5127159.
7. Goyal A, Ganjian E, Pouya HS, Mark Tyrer M. Inhibitor efficiency of migratory corrosion inhibitors to reduce corrosion in reinforced concrete exposed to high chloride environment. Constr Build Mater. 2021;303:124461.
8. Brueckner R, Cobbs R, Atkins C. A review of developments in cathodic protection systems for reinforced concrete structures. MATEC Web Conf. 2022;361:02001. https://doi.org/10.1051/matecconf/202236102001
9. Yeomans S. Galvanized steel reinforcement in concrete. Amsterdam: Elsevier; 2004.
10. De La Fuente D, Castaño JG, Morcillo M. Long-term atmospheric corrosion of zinc. Corros Sci. 2007;49(3):1420-36. http://doi.org/10.1590/S0100-40422006000100004.
11. Musters TH, Bradbury A, Trinchi A, Cole IS, Markley T, Lau D, et al. The atmospheric corrosion of zinc: the effects of salt concentration, droplet size and droplet shape. Electrochim Acta. 2011;56(4):1866-73.
12. Oliveira M. Investigação do ácido etanodióico na formação de filmes superficiais sobre zinco e avaliação do efeito destes filmes na resistência à corrosão [thesis]. São Paulo: Universidade de São Paulo; 2017.
13. Pokorný P, Tej P, Kouřil M. Evaluation of the impact of corrosion of hot-dip galvanized reinforcement on bond strength with concrete: a review. Constr Build Mater. 2017;132:271-89. http://doi.org/10.1016/j.conbuildmat.2016.11.096.
14. Tomachuk CR, Elsner CI, Di Sarli AR, Ferraz OB. Corrosion resistance of Cr (III) conversion treatments applied on electrogalvanized steel and subjected to chloride containing media. Mater Chem Phys. 2010;119(1-2):19-29. http://doi.org/10.1016/j.matchemphys.2009.07.041.
15. Arenas MA, Casado C, Nobel-Pujol V, De Damborenea J. Influence of the conversion coating on the corrosion of galvanized reinforcing steel. Cement Concr Compos. 2006;28(3):267-75. http://doi.org/10.1016/j.cemconcomp.2006.01.010.
16. Magalhães AAO, Margarit ICP, Mattos OR. Electrochemical characterization of chromate coatings on galvanized steel. Electrochim Acta. 2009;44:4281-7. http://doi.org/10.1016/S0013-4686(99)00143-7.
17. Haney JT Jr, Erraguntla N, Sielken RL Jr, Valdez-Flores C. Development of an inhalation unit risk factor for hexavalent chromium. Regul Toxicol Pharmacol. 2014;68:201-11. http://doi.org/10.1016/j.yrtph.2013.12.005.
18. Pokorný P. Efficiency of conversion coatings against activation of galvanized steel in model concrete pore solutions. Koroze a Ochrana Materiálu. 2014;57(4):115-26. http://doi.org/10.2478/kom-2013-0014.
19. Trindade GF. Dicarboxylic acids analyzed by time-of-flight secondary ion mass spectrometry. Part 0: ethanedioic acid. Surf Sci Spectra. 2017;24(021401). http://doi.org/10.1116/1.5016318.
20. Ferreira JM Jr, Oliveira M, Trindade GF, Santos LCL, Tomachuk CR, Baker MA. Development and characterization of zinc oxalate conversion coatings on zinc. Corros Sci. 2018;137:13-32. http://doi.org/10.1016/j.corsci.2018.03.011.
21. Giacomelli C, Giacomelli FC, Baptista JAA, Spinelli A. The effect of oxalic acid on the corrosion of carbon steel. Anti-Corros Methods Mater. 2004;51(2):105-11. http://doi.org/10.1108/00035590410523193.
22. Rammelt U, Koehler S, Reinhard G. Electrochemical characterization of the ability of dicarboxylic acid salts to inhibit the corrosion of mild steel in aqueous solutions. Corros Sci. 2011;53(11):3515-20. http://doi.org/10.1016/j.corsci.2011.06.023.
23. Ferreira JM Jr, Rossi JL, Baker MA, Hinder SJ, Costa I. Deposição e caracterização de um novo revestimento misto orgânico/inorgânico contendo cério para proteção contra corrosão de aço eletrogalvanizado. Int J Electrochem Sci. 2014;9:1827-39.
24. Ferreira JM Jr, Souza KP, Queiroz FM, Costa I, Tomachuk CR. Caracterização eletroquímica e química de superfícies de zinco eletrodepositadas expostas a novos tratamentos superficiais. Surf Coat Tech. 2016;294:36-46.
25. Ferreira JM Jr, Souza KP, Rossi JL, Costa I, Trindade GF, Tomachuk CR. Proteção contra corrosão de aço eletrogalvanizado por tratamentos superficiais contendo compostos de cério e nióbio. Int J Electrochem Sci. 2016;11:6655-72.
26. Cedrim FA, Almeida VLSD, Souza CACD, Lima PRL, Jesus MDD, Ribeiro DV. Corrodibility and adherence of reinforced concrete rebars electroplated with zinc and zinc-nickel alloys. Mater Res. 2019;22(4)
27. ACI Committee 440. Guide for the design and construction of structural concrete reinforced with FRP bars (ACI 440.1R-06). Farmington Hills: American Concrete Institute; 2006.
28. NACE International. NACE Standard RP0775-2005: preparation, installation, analysis, and interpretation of corrosion coupons in oilfield operations. Houston: NACE; 2005.

29. Yoo JD, Ogle K, Volovitch P. The effect of synthetic zinc corrosion products on corrosion of electrogalvanized steel. II. Zinc reactivity and galvanic coupling zinc/steel in presence of zinc corrosion products. Corros Sci. 2013;83:32-7. http://doi.org/10.1016/j.corsci.2013.12.024.
30. Bellezze T, Malavolta M, Quaranta A, Ruffini N, Roventi G. Corrosion behaviour in concrete of three differently galvanized steel bars. Cement Concr Compos. 2006;28(3):246-55. http://doi.org/10.1016/j.cemconcomp.2006.01.011.
31. Pereira MS, Barbosa LL, Souza CAC, de Moraes ACM, Carlos IA. The influence of sorbitol on zinc film deposition, zinc dissolution process and morphology of deposits obtained from alkaline bath. J Appl Electrochem. 2006;36:727-32. http://doi.org/10.1007/s10800-006-9133-z.
32. Ribeiro DV, Abrantes JCC. Application of electrochemical impedance spectroscopy (EIS) to monitor the corrosion of reinforced concrete: a new approach. Constr Build Mater. 2016;111:98-104. http://doi.org/10.1016/j.conbuildmat.2016.02.047.
33. Bellezze T, Malavolta M, Quaranta A, Ruffini N, Roventi G. Corrosion behaviour in concrete of three differently galvanized steel bars. Cement Concr Compos. 2012;28(3):246-55.
34. Roventi G, Bellezze T, Barbaresi E, Fratesi R. Effect of carbonation process on the passivating products of zinc in Ca(OH)2 saturated solution. Materials and Corrosion. 2013;64(11):1007-14.
35. Shamsipur M, Roushani M, Pourmortazavi SM. Electrochemical synthesis and characterization of zinc oxalate nanoparticles. Mater Res Bull. 2013;48(3):1275-80. http://doi.org/10.1016/j.materresbull.2012.12.032.
36. Khorsand M, Mouanga M, Bercot P, Rauch JY. Comparison of corrosion behaviour of zinc in NaCl and in NaOH solutions. Part I: corrosion layer characterization. Corros Sci. 2010;52(12):3984-92. http://doi.org/10.1016/j.corsci.2010.08.003.
37. Román J, Vera R, Bagnara M, Carvajal AM, Aperador W. Effect of chloride ions on the corrosion of galvanized steel embedded in concrete prepared with cements of different composition. Int J Electrochem Sci. 2014;9(2):580-92. http://doi.org/10.1016/S1452-3981(23)07741-6.